

## FLOW MEASUREMENT AROUND A NON-CIRCULAR TUBE

Nouri-Borujerdi A.\* and Lavasani A.

\*Author for correspondence

\*Islamic Azad University, South Tehran Branch  
 Islamic Azad University, Science & Research Branch  
 Tehran, Iran  
 E-mail: nouriba@yahoo.com

### ABSTRACT

The flow behavior around a cam shaped tube in cross flow has been investigated experimentally using flow visualization and pressure distribution measurement. The range of angle of attack and Reynolds number based on an equivalent circular tube are within  $0 \leq \alpha \leq 360^\circ$  and  $2 \times 10^4 < Re_{eq} < 3.4 \times 10^4$ , respectively.

The pressure drag features are clarified in relation to the flow behavior around the tube. It is found that the highest pressure drag coefficient occurs at  $\alpha = 90^\circ$  and  $270^\circ$  over the whole range of Reynolds number. Results show that the pressure drag coefficient of the cam shaped tube is lower than that of a circular tube with the same surface area for more of the angles of attack.

### INTRODUCTION

The exploitations of high performance heat exchangers for saving and making effective use of energy is a very important and urgent problem. Among many types of heat exchangers, those constructed of non-circular tubes have been used in many industries [1-13]. Major objectives in the design of these heat exchangers could be reduction of pressure drop and fouling for a given amount of heat transferred.

Ota et al. [1] investigated experimentally the thermal performance of a single elliptical cylinder with an axis ratio (major axis to minor axis) of 2 in a flow of air having Reynolds numbers of  $5000 < Re_c < 90000$  with angles of attack  $0 < \alpha < 90^\circ$ .  $Re_c$  is the Reynolds number based on the major axis  $c$ . For air flow parallel to the major axis, they found that the Nusselt number for the elliptical cylinder was higher than that obtained for a circular cylinder from an empirical correlation.

Ota et al. [2] tested an elliptical cylinder with an axis ratio of 3 with  $8000 < Re_c < 79000$ . The Nusselt number for the elliptical cylinder was found to be higher than that for a circular cylinder.

For tube bundles, Merker and Hanke [3] found experimentally the heat transfer and pressure drop performance of staggered oval tube bundles with different transversal and longitudinal spacing. The oval tube axis ratio was 3.97. They showed that an exchanger with oval-shaped tubes had smaller frontal areas on the shell-side compared to those with circular tubes.

Ota and Nishiyama [4] investigated experimentally the flow around two elliptical cylinders with axis ratio 3 in a tandem arrangement. The static pressure distribution on the surface was measured and the drag, lift, and moment coefficients were evaluated for a range of angles of attack and cylinder spacing.

Prasad et al. [5] reported heat transfer and pressure drop from an airfoil in cross flow. Their aerofoil test section was the NACA-0024 and they concluded that this shape gives lower values of  $C_f/St$  compared to the circular tube.

Kondjoyan and Daudin [6] studied experimentally the effect of variation in the free stream turbulence intensity from 1.5% to 40% on the heat transfer from a circular cylinder and an elliptical cylinder with axis ratio 4 for Reynolds numbers between  $3 \times 10^3 < Re_D < 4 \times 10^4$ .  $Re_D$  is based on the diameter of an equivalent circular cylinder for an elliptical cylinder. Their conclusion was that turbulence intensity effect is as important as air velocity effect. They indicated that the Nusselt number for the elliptical cylinder was about 14% lower than that for the equivalent circular cylinder.

Salazar et al. [7] measured the heat transfer from a bank of elliptical tubes in a cross-flow. The elliptical tube axis ratios used were 1.054, 1.26, and 1.44. The characteristic length in  $Re$  and  $Nu$  for the elliptical tube was assumed to be equal to the minor axis. The results indicated that correlations of circular tubes were slightly higher than the measurements of the elliptical tubes.

Badr [8] reported the forced convection heat transfer from a straight isothermal tube of elliptic cross-section placed in a uniform air stream. In this study, the Reynolds number range is  $20 < Re < 500$  and angles of inclination is  $0^\circ < \alpha < 90^\circ$ . The tube

axis ratio varies between 0.4 and 0.9. His results also show that the rate of heat transfer reaches its maximum value at  $\alpha=0^\circ$  while the minimum occurs at  $\alpha=90^\circ$ .

For evaporatively cooled heat exchangers, Hasan and Sirén [9] showed that a bank of wet oval tubes has a better combined thermal-hydraulic performance than corresponding circular tubes.

Tiwari et al. [10] reported a three-dimensional computational study of forced convection heat transfer to determine the flow structure and heat transfer in a rectangular channel with a built-in oval tube and delta wing type vortex generators in various configurations. Their results indicate that vortex generators in conjunction with the oval tubes show definite promise for the improving fin-tube heat exchangers.

Matos et al. [11] studied the numerical and experimental heat transfer rate between staggered arrangements of circular and elliptic of finned tubes bundle and external flow. They have reported that the optimal elliptic arrangement exhibits a heat transfer gain of up to 19% compared to the optimal circular tube arrangement. The results illustrate that the heat transfer gain and the relative total mass reduction of up to 32% show that the elliptical arrangement has the potential to deliver considerably higher global performance and lower cost.

Heat transfer rates of shaped tubes were characterized by treating the tubes as a base circular tube to which longitudinal fin(s) by Numerical method [12]. The approach was illustrated for three streamlined shapes with fins of lenticular and oval profile. They highlighted the effects of the geometry and the Biot number on the tube efficiency and heat transfer enhancement. Convective heat transfer is enhanced for the oval shaped tube for  $2000 < Re < 20,000$  when  $Bi < 0.3$ . The potential benefit of reduced form drag remains.

Bouris et al. [13] proposed tube cross-section was a parabolic upstream shape and a semi-circular one downstream. They carried out experiments and numerical simulations on the novel tube bundle heat exchanger for studying the thermal, hydraulic and fouling characteristics. Their results indicate that they attain higher heat transfer levels with a 75% lower deposition rate and 40% lower pressure drop.

In the previous [5] and recent [12,13] studies, a non circular tube with cross-section similar to a cam was used in a heat exchanger for increasing thermal-hydraulic performance and reducing of fouling. Therefore, the flow characteristics around a cam shaped tube at different angles of attack have not been investigated. In this study, the flow visualization around this tube at  $0 \leq \alpha \leq 360^\circ$  has been investigated experimentally.

## NOMENCLATURE

$C_p$	[ ]	pressure coefficient, $(p - p_\infty) / 0.5\rho U_\infty^2$
$D$	[m]	large diameter, circular tube diameter
$d$	[m]	small diameter
$L$	[m]	tube length
$l$	[m]	distance between centres
$Nu$	[ ]	Nusselt number

$P$	[Pa]	circumferential length of the cam
$Re$	[ ]	Reynolds number,
$S$	[m <sup>2</sup> ]	surface length from leading edge, distance
$U$	[m/s]	velocity

### Greek Letter

$\alpha$	[ ]	angle attack
$\rho$	[kg/m <sup>3</sup> ]	density

### Superscripts

---	[ ]	mean
-----	-----	------

### Subscripts

eq	[ ]	equivalent
$\infty$	[ ]	free-stream

## EXPERIMENTAL APPARATUS AND MEASUREMENT

A small wind tunnel, as shown in Figure 1, was built to carry out these experiments. The tunnel was an open tunnel with air drawn through it by a 1.5 kw fan. A deep aluminium honeycomb at entrance smoothed the flow and reduced or eliminated fluctuations. The working section measured 0.30-m high by 0.35-m wide.

The cross-section of the test tube is shown schematically in Fig. 1. This tube is similar a cam shaped that comprises two circles with diameters of  $d$  and  $D$ , and their centres are located on a straight line with a distance of  $l$  apart. The test tube is made of commercial copper plate with 0.3 mm thickness and a length of 120 mm. Three test tubes were used for investigation of the effect of tube dimensions on the flow characteristics. The dimensions of each tube are given in Table 1. Its surface of each tubes are covered with 20 holes (1 mm in diameter) drilled to measure the static pressure on the tube surface by a dial manometer.

A pitot static tube was used for measuring velocity distribution by traversing the tube across the cross-section of test section. The air velocity in front of the test section can be varied from 12.5 to 21.5 m/s by controlling a variable speed motor. During experiments, the temperature variation in test section was less than 1°C.

The angle of attack was varied from  $0 \leq \alpha \leq 360^\circ$  in order to clarify variations of the flow characteristics of the tube with it. In the present paper,  $\alpha$  is angle between of the major axis of the cam shape tube with the direction of the upstream uniform flow. The angle of attack has positive values on clock wise rotation.

The tunnel blockage ratio at  $\alpha = 90^\circ$  are more than of another angles of attack. This ratio varied from 0.09 to 0.27 for tube No.1 and No.3, respectively. In present paper, however, no corrections were made for the tunnel wall effects upon the flow characteristics.

To estimate the pressure drag of the cam shaped tube compared to that of a circular tube with various cross sections, it is important to select an appropriate reference length.  $D_{eq}$  is the diameter of an equivalent circular tube whose circumferential length is equal to that of the cam-shaped tube.

The  $L/D_{eq}$  ratios for three tubes of table.1 are 4.85, 3.36 and 2.03 respectively. This ratio has not effects on drag coefficient

ang

for  $L/D_{eq} = \infty$  so the effect of this ratio on this coefficient for first, second and third tube is 38.3%, 39.7% and 43.3%, respectively [14]. For  $L/D_{eq} > 4$  this ratio has little effects on heat transfer so the effect of this ratio on heat transfer from second and third tube with  $1.5 \times 10^4 < Re_{eq} < 4.8 \times 10^4$  is 4-6% and 6-10% respectively [15]. In the present paper, however no corrections were made for  $L/D_{eq}$  effects.

The pressure drag coefficient  $C_D$  is determined experimentally from pressure distribution over the cam shaped-tube surface, including the large and small circles as well as two tangent lines between them as follows.

$$C_D = \frac{1}{D_{eq}} \oint C_p \cos \psi \, ds = \frac{1}{D_{eq}} \left\{ \sum_{i=1}^{20} C_{p,i} \cos \psi_i \Delta S_i \right\} \quad (1)$$

As shown in Figure 2,  $\psi$  is different for each of the holes. This angle denotes the angle between the normal vector on the tube surface and free stream. The angle  $\psi$  is changed with respect to the angle of attack.  $S$  denotes the surface distance from leading edge of the cylinder and  $\Delta S_i$  represents a length on the tube perimeter belong to each hole.

The error in measuring the pressure drag coefficient for the cam shaped tube can easily be obtained by differentiation of Eq. (1) and the final result will be as follows:

$$\Delta(C_D) = C_D \left\{ \left( \frac{\Delta(D_{eq})}{D_{eq}} \right)^2 + \sum_{i=1}^{20} \left[ \left( \frac{\Delta(C_{p,i})}{C_{p,i}} \right)^2 + \left( \frac{\Delta(\psi_i)}{\cotg \psi_i} \right)^2 + \left( \frac{\Delta(\Delta S_i)}{S_i} \right)^2 \right] \right\}^{0.5} \quad (2)$$

where  $\Delta(D_{eq})$  is measurement error of equivalent diameter with value of about  $\pm 0.0005 \, m$  making that  $\Delta(D_{eq})/D_{eq}$  for tube No.1 of table.1 is about 2%.  $\Delta(C_{p,i})$ ,  $\Delta(\psi_i)$  and  $\Delta(\Delta S_i)$  are respectively the measurement errors of the pressure coefficient, angle of  $\psi_i$  and length on the tube perimeter. Errors in the pressure coefficient can be obtained by  $\Delta(C_{p,i}) = C_{p,i} \left[ (\Delta P / (P - P_\infty))^2 + (\Delta(\rho_a) / \rho_a)^2 + (2 \Delta U / U)^2 \right]^{0.5}$ , where  $\Delta(\rho_a)$  and  $\Delta(U)$  are the errors of the density and velocity of air. This value is about 3.8 to 10% of  $C_{p,i}$  for different velocities. The density of air is function of the air temperature. These functions can be obtained from the air physical properties [16]. These errors can be estimated as,  $\Delta(\rho_a) = |d\rho_a/dT_a| \Delta(T_a)$ . Using the tables of the thermodynamic properties of air, the density gradients with respect to the temperature can easily be obtained in the range of the temperature variations. This value is about 0.03% of  $\rho_a$ .  $\Delta(U)$  is measurement error of velocity with value of about  $\pm 0.01$  making that  $\Delta(U)/U$  to be about 0.04 to 0.07%.

Substituting the above-mentioned errors in Eq. (2), the pressure drag coefficient uncertainty for tube No.1 and  $0 \leq \alpha \leq 360^\circ$  are about 14.4 to 15.7 percent.

## PROCESSING OF RESULTS

A single circular tube with diameter of 2.47 cm and length of 12.5 cm is tested before testing the cam shaped-tube, to verify the data-taking process and to check the related equipment setup. The difference between the present results and that of curve-fit formula by White [14] is about 1-2 percent.

It can, therefore, be concluded that the set up can be used for flow visualization and measuring pressure drag from a cam shaped tube.

Representative examples of the flow visualization around tube No.1 at  $180 \leq \alpha \leq 360^\circ$  are demonstrated in Figure 2. The boundary layer separation is varies with angle of attack. An increase of the angle of attack brings on a decrease of the flow velocity oncoming to the upstream surface of the tube. Furthermore, the wake width is relatively small and then, in the separated flow region, a transversal motion of the fluid may be suppressed. Angle of attack of  $270^\circ$  brings about a much wider wake behind the tube and the transversal motion of the fluid is very violent therein. Consequently the tube surface is washed out frequently by the fluid entrained from the main flow.

The flow and heat transfer characteristics of the cam shaped tube are closely related to boundary layer separation [17] and varies with angle of attack. Variation of the  $C_D$  and  $\overline{Nu}_{eq}$  with  $\alpha$  for tube No.1 are shown in Figure 3. The shape of drag coefficient curve is repeated every other  $150^\circ$ . The minimum drag coefficients and Nusselt number are belonging to  $\alpha = 30^\circ$  and  $\alpha = 330^\circ$ . As described previously, a decrease in the oncoming flow velocity to the upstream surface of the tube brings about a relatively low value of drag coefficients and Nusselt number therein. On the other hand,  $C_D$  and  $\overline{Nu}_{eq}$  at  $\alpha = 90^\circ$  and  $270^\circ$  is highest over the whole Reynolds number range examined in the present work. At large angles of attack the pressure inside the separated flow region is very low. Such a low pressure and large wake downstream of the tube may bring about a violent motion of fluid therein and it results in a very high drag coefficient as demonstrated previously. It is to be noted that the present value of  $C_D$  and  $\overline{Nu}_{eq}$  is based upon the equivalent diameter as the reference length.

The flow characteristic of the cam shaped tube varies with  $d/D$  and  $l/D$  ratio. The effect of  $l/D$  ratio on the drag coefficient for same  $d/D$  is studied by considering the case of  $\alpha = 0$  and  $360^\circ$  for  $U = 15 \, m/s$ . Variations of this coefficient with  $\alpha$  for three cam shaped tubes are shown in Figure 4. The value of  $C_D$  for  $l/D = 3$  at  $\alpha = 0, 180$  and  $360^\circ$  is very low compared with the other tubes. As shown in the figure, at angles in which the tube is horizontal ( $\alpha = 0, 180$  and  $360^\circ$ ), the drag coefficient of more narrow tubes decreases but with increase in angles of attack the coefficient increases. So that at  $\alpha = 0, 180$  and  $360^\circ$  the drag coefficient of tube with  $l/D = 0.5$  is about 2 and 6.5 times of this

coefficient for tubes with  $l/D=1.3$  and  $l/D=3$ . But at  $\alpha=90$  and  $270^\circ$  these ratios are 0.74 and 0.85 respectively.

From Figure 4., It can be compared between pressure drag coefficient of three cam shaped-tubes with  $D_{eq}=24.7, 35.7$  and  $59.1$  mm for  $\alpha=0^\circ$  to  $360^\circ$  and three circular tubes having the same circumferential length ( $D=24.7, 35.7$  and  $59.1$  mm) with drag coefficient  $C_D=0.74, 0.72$  and  $0.68$  [14], respectively. Pressure drag coefficient of the cam shaped-tube for any angles of attack is lower than that of circular tube with same circumferential length except for angles of attack of  $60$  to  $90$  and  $240$  to  $300$ . The minimum amount of drag coefficient for cam shaped tube, which occurs at  $0^\circ$  and  $180^\circ$ , is about 0.1-0.7 of this amount for circular tube with similar surface area. The maximum amount of drag coefficient for cam shaped tube occurs at  $\alpha=90^\circ$  and  $270^\circ$  which is about 1.1-1.7 of this amount for circular tube with similar surface area. The minimum of this ratio occurs at  $\alpha=0^\circ$  and  $180^\circ$  and the maximum occurs at  $\alpha=90^\circ$  and  $270^\circ$  for more narrow tubes.

## CONCLUSIONS

Flow visualization and distribution pressure have been carried out on a cam shaped tube in cross flow. The angle of attack is varied  $0^\circ < \alpha < 360^\circ$  over the  $2 \times 10^4 < Re_{eq} < 3.4 \times 10^4$ .

The experiments aimed to ascertain the effects of the angle of attack and  $l/D$  over pressure drag. These Results show that pressure drag for a cam shaped tube is maximum at about  $\alpha=90^\circ$  and  $270^\circ$ .

In order to compare the available pressure drag values of cam shaped and circular cross-sections with same circumferential length, a Reynolds number based on the equivalent tube diameter has been defined. These comparisons have shown that cam shaped tubes give lower values of  $C_D$  than the circular cross-section for more of the angles of attack.

Effects of the  $l/D$  for a cam shaped tube with same  $d/D$  upon its  $C_D$  are also investigated. These results show that for tube with large  $l/D$  this coefficient is a minimum at  $\alpha=0$  and  $180^\circ$  and is a maximum at  $\alpha=90^\circ$  and  $270^\circ$ .

## REFERENCES

- [1] Ota, T., Aiba, S., Tsuruta, T. and Kaga, M., "Forced Convection Heat Transfer from an Elliptic Cylinder of Axis Ratio 1:2", Bulletin of JSME, 26 (212) (1983) 262–267.
- [2] Ota, T., Nishiyama, H., Taoka, Y., "Heat transfer and flow around an elliptic cylinder", International Journal of Heat and Mass Transfer, 27 (10) (1984) 1771–1779.
- [3] Merker, G. P., Hanke, H., "Heat transfer and pressure drop on the shell-side of tube-banks having oval-shaped tubes", International Journal of Heat and Mass Transfer, 29 (12) (1986) 1903–1909.
- [4] Ota, T., Nishiyama, H., "Flow around two elliptic cylinders in tandem arrangement", Journal of Fluids Engineering, Transactions of the ASME, 108 (1) (1986) 98–103.
- [5] Prasad, B.V.S.S.S., Tawfek, A.A. and Rao, V.R.M., Heat Transfer from Aerofoils in Cross-Flow, International Communications in Heat and Mass Transfer, 19, (1992) 870-890.
- [6] Kondjoyan, A., Daudin, J. D., "Effects of free stream turbulence intensity on heat and mass transfer at the surface of a circular cylinder and an elliptical cylinder axis ratio 4", International Journal of Heat and Mass Transfer, 38 (10) (1995)1735–1749.
- [7] Salazar, E., Gonzalez, J. J., Lopez De Ramos, A., Pironti, F., Gonzalez-Mendizabal, D., "Evaluation of the heat transfer coefficient in a bank of elliptic tubes", American Institution of Chemical Engineers, AIChE Symposium Series, Heat Transfer,314 (1997) 185 – 190.
- [8] Badr, H. M., "Force convection from a straight elliptical tube", Journal of Heat and Mass Transfer, 34 (1998) 229-236.
- [9] Hasan, A., Sirén, K., "Performance investigation of plain circular and oval tube evaporatively-cooled heat exchangers", Applied Thermal Engineering, 24 (5-6) (2004) 777–790.
- [10] Tiwari, S., Maurya, D., Biswas, G. and Eswaran, V., Heat transfer enhancement in cross-flow heat exchangers using oval tubes and multiple delta winglets, International Journal of Heat and Mass Transfer, 46, (2003) 2841–2856.
- [11] Matos, R.S., Laursen, T.A., Vargas, J.V.C. and Bejan, A., Three-dimensional optimization of staggered finned circular and elliptic tubes in forced convection, International Journal of Thermal Sciences, 43, (2004) 477–487.
- [12] Zhihua., Davidson, Jane H. and Mantell, Susan C., "Heat Transfer Enhancement Using Shaped Polymer Tubes :Fin Analysis," Journal of Heat Transfer , 126 (2004), 211-218
- [13] Bouris, D., Konstantinidis, E., Balabani, S., Castiglia, D., Bergeles, G., Design of a novel, intensified heat exchanger for reduced fouling rates, International Journal of Heat and Mass Transfer 48 (2005) 3817–3832.
- [14] White, F., Fluid Mechanics, Mc Graw-Hill, New York, 2005.
- [15] Quarmby, A., and AL-Fakhri, A. A. M., " Effect of Finite Length on Forced Convection Heat Transfer from Cylinder" Int.J.Heat Mass transfer, 23 (1980) 463-469.
- [16] Netcati Ozisik, M., Heat transfer, Mc Graw-Hill, New York, 1985.
- [17] Douglas, J.F., Gasiorek, J.M., Swaffield, J.A., Fluid Mechanics, Longman Scientific&Technical, New York, 1990.

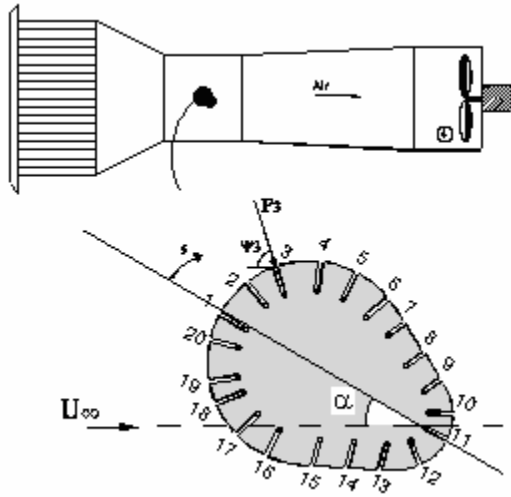


Figure 1 Wind tunnel layout

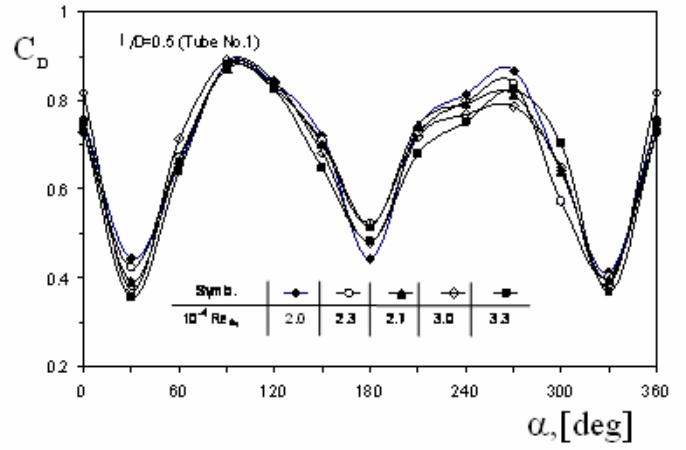


Figure 3 Pressure drag coefficient vs. angle of attack for Reynolds number

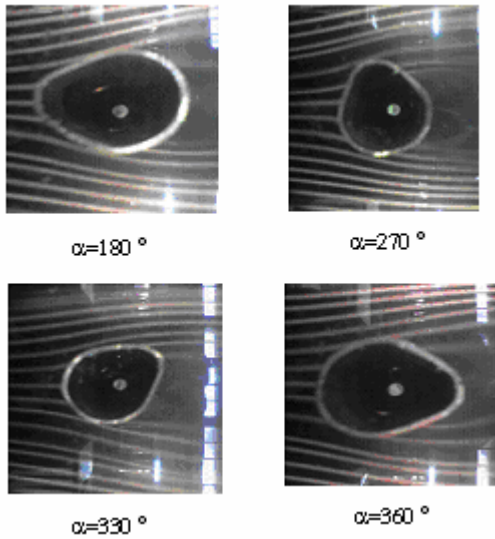


Figure 2 Flow visualization around a cam Shaped-tube with  $l/D=0.5$

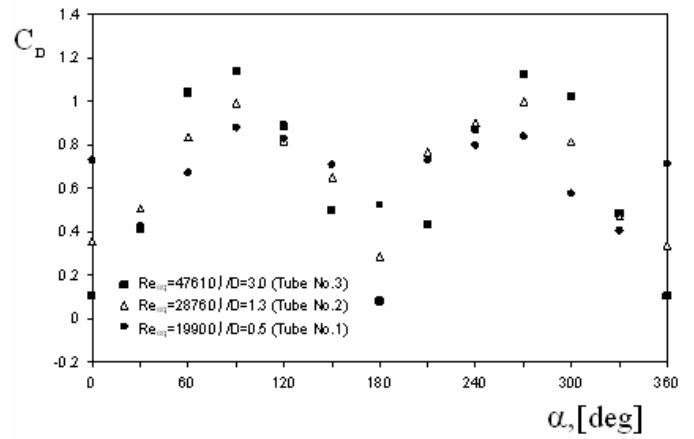


Figure 4 Drag coefficient vs. angle of attack for different  $l/D$